Nonlinear evolution and runup–rundown of long waves over a sloping beach

By UTKU KÂNOĞLU

Department of Engineering Sciences, Middle East Technical University, 06531 Ankara, Turkey

The initial value problem of the nonlinear evolution, shoreline motion and flow velocities of long waves climbing sloping beaches is solved analytically for different initial waveforms. A major difficulty in earlier work utilizing hodograph-type transformation when solving either boundary value or initial value problems has been the specification of equivalent boundary or initial condition in the transformed space. Here, in solving the initial value problem, the transformation is linearized in space at $t = 0$, then the full nonlinear transformation is used to solve the initial value problem of the nonlinear shallow-water wave equations. A solution method is presented to describe the most physically realistic initial waveforms and simplified equations for the runup–rundown motions and shoreline velocities. This linearization of the initial condition does not appear to affect the subsequent nonlinear evolution, as shown through comparisons with earlier studies. Comparisons with runup results from solutions of the boundary value problem suggest the same variation with the runup laws. The methodology presented here appears simpler than earlier work as it does not involve the numerical calculation of singular elliptic integrals.

1. Introduction

The nonlinear evolution of a wave over a sloping beach is theoretically and numerically challenging due to the moving boundary singularity. Yet, it is important to have a good estimate of the shoreline velocity and associated runup–rundown motion, since they are crucial for the control of coastal flooding and planning of coastal structures.

The major analytical advance in the nonlinear shallow-water wave equations on a uniformly sloping beach was presented by Carrier & Greenspan (1958), known as the Carrier–Greenspan transformation. They outlined a hodograph transformation using the Riemann invariants of the hyperbolic system to reduce the nonlinear shallow-water wave equations to a single second-order linear equation. Even though the Carrier–Greenspan transformation is widely used, there are two major difficulties with it which will be discussed in §2. Tuck & Hwang (1972) suggested a slightly different transformation which not only linearizes the nonlinear shallow-water wave equations but also turns them into forms similar to their linear forms. In a recent study, Carrier, Wu & Yeh (2003) developed the Green function representation of the solution of the nonlinear shallow-water wave equations using the transformation given by Tuck & Hwang (1972). They were able to evaluate the Green function explicitly and obtained the complete elliptic integral of the first kind, which is highly singular. Nonetheless, they solved the nonlinear propagation problem for arbitrary initial waveform employing numerical integration.
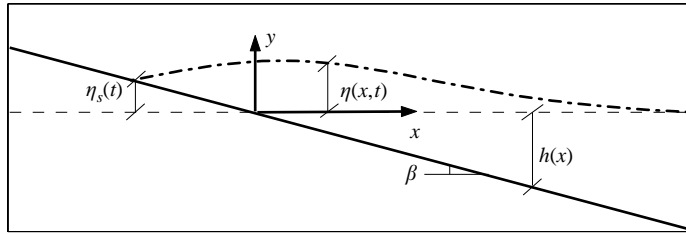
FIGURE 1. Definition sketch.

Pelinovsky (1995) developed analytical solutions to the nonlinear shallow-water wave equations and discussed their relation to Carrier & Greenspan (1958). Synolakis (1987) and Tadepalli & Synolakis (1994) considered a canonical problem: propagation over a constant-depth segment connected to a uniformly sloping beach. While Synolakis (1987) considered solitary wave propagation, Tadepalli & Synolakis (1994) defined a new type of wave now commonly known as N-waves. Both studies considered the linear shallow-water wave equation and provided analytical expressions for the maximum runup. In addition, Synolakis (1987) solved the nonlinear canonical boundary value problem for solitary wave propagation using the Carrier–Greenspan transformation, specifying the boundary condition at the toe of the beach from the equivalent linear problem. Synolakis (1987) used the linearized form of the hodograph transformation for the spatial and temporal variables to specify the boundary condition. Despite the linearization used to specify the boundary condition, the subsequent analytical solution maintains the nonlinear effects as shown by Synolakis (1987) and Titov & Synolakis (1995) through comparisons with laboratory data and numerical predictions respectively.

In this paper, it is proposed that any initial waveform can first be represented in the transform space using the linearized form of the Carrier–Greenspan transformation for the spatial variable, then the nonlinear evolutions of these initial waveforms can be directly evaluated. The integrals for the shoreline motion and velocity are simplified substantially. This approach is applied to the Gaussian and leading-depression N-wave initial forms presented by Carrier *et al.* (2003) and results are compared. The method is also extended to the different N-wave initial forms presented by Tadepalli & Synolakis (1994) and some observations are made regarding the similar trends in the maximum runup in the results of Tadepalli & Synolakis (1994) and the present study.

2. General formulation

The one-plus-one dimensional nonlinear shallow-water wave equations that describe propagation over undisturbed water of variable depth $h(x)$ (see figure 1) are

$$u_t + uu_x + \eta_x = 0, \quad [u(h+\eta)]_x + \eta_t = 0, \qquad (2.1a, b)$$

where $u(x, t)$ and $\eta(x, t)$ are the horizontal depth-averaged velocity and free-surface elevation respectively. The origin of the coordinate system is chosen at the initial shoreline with x increasing in the seaward-direction and $\tilde{h}(\tilde{x}) = \tilde{x} \tan \beta$ where β is the beach angle from the horizontal. Using the reference length $\tilde{l}$, the dimensionless variables are $x = \tilde{x}/\tilde{l}$, $h = \tilde{h}/(\tilde{l} \tan \beta)$, $\eta = \tilde{\eta}/(\tilde{l} \tan \beta)$, $u = \tilde{u}/(\tilde{g}\tilde{l} \tan \beta)^{1/2}$, and $t = \tilde{t}(\tilde{g} \tan \beta/\tilde{l})^{1/2}$ where $\tilde{g}$ is the gravitational acceleration. Carrier & Greenspan (1958) outlined a hodograph transformation defining a new set of independent variables (σ, λ) and reduced the nonlinear shallow-water wave equations to the

single second-order linear equation

$$\sigma\phi_{\lambda\lambda} - (\sigma\phi_\sigma)_\sigma = 0, \tag{2.2}$$

using the Riemann invariants of the hyperbolic system (2.1*a*, *b*). The potential $\phi(\sigma, \lambda)$ was introduced as $u = \phi_\sigma/\sigma$. The Carrier–Greenspan transformation not only reduces the nonlinear shallow-water wave equations to a second-order linear equation, but also fixes the instantaneous shoreline to $\sigma = 0$ in (σ, λ)-space. Furthermore, a bounded solution at the shoreline combined with given initial conditions at $\lambda = 0$, $u = 0$ and a wave profile in (σ, λ)-space, $\eta(\sigma, 0)$, implies the following solution in the transform space:

$$\phi(\sigma, \lambda) = -\int_0^\infty \int_0^\infty \frac{1}{\omega} \xi^2 \Phi(\xi) J_0(\omega\sigma) J_1(\omega\xi) \sin(\omega\lambda) \, d\omega \, d\xi, \tag{2.3}$$

where $\Phi(\sigma) = u_\lambda(\sigma, 0) = 4\eta_\sigma(\sigma, 0)/\sigma$. Once $\phi(\sigma, \lambda)$ is known, the following hodograph transformation can be used to obtain the solution in (x, t)-space:

$$u = \frac{\phi_\sigma}{\sigma}, \quad \eta = \tfrac{1}{4}\phi_\lambda - \tfrac{1}{2}u^2, \quad x = \tfrac{1}{16}\sigma^2 - \tfrac{1}{4}\phi_\lambda + \tfrac{1}{2}u^2, \quad t = u - \tfrac{1}{2}\lambda. \tag{2.4a, b, c, d}$$

Carrier & Greenspan (1958) left their formulation here and considered two very specific initial wave profiles, since generalization to realistic profiles was perhaps less obvious. The difficulty lies in the derivation of an equivalent initial condition over the transform (σ, λ)-space for a given initial wave profile in the physical (x, t)-space. Even though the solution can be obtained in (σ, λ)-space using (2.4*a*, *b*) and can be converted to the solution in (x, t)-space through (2.4*c*, *d*), another problem with this transformation is deriving a solution for a particular time t^* or at a particular location x^*. The former difficulty will be resolved in the present study, while the latter was resolved by Synolakis (1987) seeking a solution either for given t^* or at given x^* using the Newton–Raphson iteration algorithms respectively:

$$\lambda_{i+1} = \lambda_i - \frac{t^* - t(\lambda_i)}{\left(-u_\lambda + \tfrac{1}{2}\right)_{\lambda_i}} \quad \text{or} \quad \sigma_{i+1} = \sigma_i - \frac{x^* - x(\sigma_i)}{\left(-\tfrac{1}{8}\sigma + \tfrac{1}{4}\phi_{\sigma\lambda} - uu_\sigma\right)_{\sigma_i}}. \tag{2.5a, b}$$

The difficulty in deriving an initial condition in (σ, λ)-space is overcome by simply using the linearized form of the hodograph transformation for the spatial variable in the definition of the initial condition. Once an initial value problem is specified in (x, t)-space as $\eta(x, 0)$, the linearized hodograph transformation $x \cong \tfrac{1}{16}\sigma^2$ is used directly to define the initial waveform in (σ, λ)-space, $\eta(\tfrac{1}{16}\sigma^2, 0)$. Thus $\Phi(\sigma) = 4\eta_\sigma(\tfrac{1}{16}\sigma^2, 0)/\sigma$ is found, and $\phi(\sigma, \lambda)$ follows directly through a simple integration as in (2.3). Then, it becomes possible to investigate any realistic initial waveform such as the Gaussian and N-wave shapes employed in Carrier *et al.* (2003) and the isosceles and general N-waves defined by Tadepalli & Synolakis (1994).

Given the initial waveform $\eta(x, 0)$, the evolution of the water-surface elevation is now given by

$$\eta(\sigma, \lambda) = \tfrac{1}{4}\phi_\lambda - \tfrac{1}{2}u^2 = -\frac{1}{4}\left\{\int_0^\infty \xi^2 \Phi(\xi)\left[\int_0^\infty J_0(\omega\sigma) J_1(\omega\xi) \cos(\omega\lambda) \, d\omega\right] d\xi\right\}$$
$$- \frac{1}{2}\left\{\int_0^\infty \xi^2 \Phi(\xi)\left[\int_0^\infty \frac{J_1(\omega\sigma)}{\sigma} J_1(\omega\xi) \sin(\omega\lambda) \, d\omega\right] d\xi\right\}^2, \tag{2.6}$$

where $\Phi(\sigma) = 4\,\eta_\sigma(\sigma, 0)/\sigma$. Equation (2.6) can be integrated numerically to obtain the water-surface elevation given t^* or x^*.

Since they are important for coastal planning, simple expressions for shoreline runup–rundown motion and velocity are useful. Considering the shoreline to correspond to $\sigma = 0$ in (σ, λ)-space, (2.6) reduces to the following equation for the runup–rundown motion:

$$\eta_s(\lambda) = \eta(0, \lambda) = \tfrac{1}{4}\phi_\lambda - \tfrac{1}{2}u_s^2 = -\frac{1}{4}\left\{\int_0^\infty \xi^2 \Phi(\xi)\left[\int_0^\infty J_1(\omega\xi)\cos(\omega\lambda)\,\mathrm{d}\omega\right]\mathrm{d}\xi\right\}$$

$$-\frac{1}{2}\left\{\int_0^\infty \xi^2 \Phi(\xi)\left[\int_0^\infty \tfrac{1}{2}\omega J_1(\omega\xi)\sin(\omega\lambda)\,\mathrm{d}\omega\right]\mathrm{d}\xi\right\}^2. \quad (2.7)$$

Here the singularity of $u = \phi_\sigma/\sigma$ at $\sigma = 0$ is removed by considering $\lim_{\sigma \to 0}[J_1(\omega\sigma)/\sigma] = \tfrac{1}{2}\omega$. Given that and taking $\lambda = -\tau^2$,

$$\int_0^\infty J_1(\omega\xi)\cos(\omega\tau^2)\,\mathrm{d}\omega = \begin{cases} \cos(\arcsin(\tau^2/\xi))/\sqrt{\xi^2 - \tau^4}, & \tau^2 < \xi, \\ \infty \text{ or } 0, & \tau^2 = \xi, \\ -\xi/[(\tau^2 + \sqrt{\tau^4 - \xi^2})\sqrt{\tau^4 - \xi^2}], & \tau^2 > \xi, \end{cases} \quad (2.8)$$

see Gradshteyn & Ryzhik (1994); integration by parts and Leibnitz's formula lead to the following simplified equation for the shoreline motion:

$$\eta_s(\lambda) = \tfrac{1}{4}\phi_\lambda - \tfrac{1}{2}u_s^2 = -\frac{1}{4}\left\{\int_0^\infty \xi\Phi(\xi)\,\mathrm{d}\xi - \tau^4\Phi(0) - \int_0^{\tau^2} \tau^2\sqrt{\tau^4 - \xi^2}\,\frac{\mathrm{d}\Phi(\xi)}{\mathrm{d}\xi}\,\mathrm{d}\xi\right\}$$

$$-\frac{1}{2}\left\{-\tau^2\Phi(0) - \frac{1}{2}\int_0^{\tau^2} \frac{2\tau^4 - \xi^2}{\sqrt{\tau^4 - \xi^2}}\,\frac{\mathrm{d}\Phi(\xi)}{\mathrm{d}\xi}\,\mathrm{d}\xi\right\}^2. \quad (2.9)$$

Numerical evaluation of (2.9) provides runup–rundown motion of the shoreline. Equation (2.9) is identical to (2.7), yet much simpler. It is obvious from (2.7) and (2.9) that the maximum runup–minimum rundown are governed by the term corresponding to $\tfrac{1}{4}\phi_\lambda$ since $u = 0$ at these extreme values. In addition, shoreline velocity u_s is also given explicitly in both equations. Note that the simplified form of (2.9),

$$\eta_s(\lambda) \cong \frac{1}{4}\int_0^{\tau^2} \tau^2\sqrt{\tau^4 - \xi^2}\,\frac{\mathrm{d}\Phi(\xi)}{\mathrm{d}\xi}\,\mathrm{d}\xi - \frac{1}{2}\left\{-\frac{1}{2}\int_0^{\tau^2} \frac{2\tau^4 - \xi^2}{\sqrt{\tau^4 - \xi^2}}\,\frac{\mathrm{d}\Phi(\xi)}{\mathrm{d}\xi}\,\mathrm{d}\xi\right\}^2, \quad (2.10)$$

provides a good estimate of the shoreline motion and velocity for the cases where $\Phi(0)$ and $\int_0^\infty \xi\Phi(\xi)\,\mathrm{d}\xi$ are small. Specific examples are provided in §3.

3. Initial conditions

The detailed evolution, shoreline velocities and runup–rundown motions of different initial wave profiles are examined here for initial profiles having zero initial velocity everywhere. This is claimed to be a good representation of tectonic tsunami generation; see Synolakis *et al.* (1997) and Carrier *et al.* (2003). The method in §2 is applied to the four cases presented by Carrier *et al.* (2003) and extreme values are compared. The method is equally applicable to any other initial waveform such as the different N-wave forms proposed by Tadepalli & Synolakis (1994). After validating the method with the Carrier *et al.* (2003) results, it will be extended to solitary and N-wave initial forms.
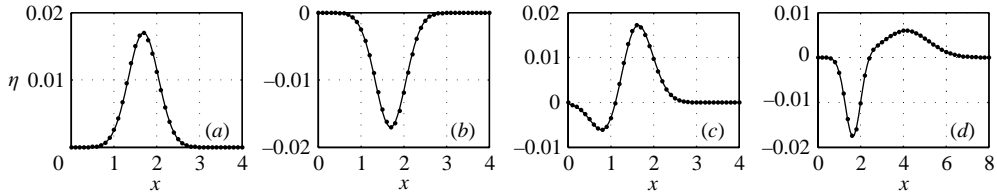
FIGURE 2. Four initial waveforms presented by Carrier *et al.* (2003). The solid lines represent proposed initial waveforms defined in (x, t)-space through (3.1) and (3.2). The nonlinear solution represented by dots is obtained with the numerical integration of (2.3) using (2.4a–d) and (2.5a) at $t^* = 0$. (a) The Gaussian initial waveform with $H_1 = 0.017$, $c_1 = 4.0$, and $x_1 = 1.69$, (b) the negative Gaussian initial waveform with $H_1 = 0.017$, $c_1 = 4.0$, and $x_1 = 1.69$, (c) the leading-depression N-wave initial form with $H_1 = 0.02$, $c_1 = 3.5$, $x_1 = 1.5625$, $H_2 = 0.01$, $c_2 = 3.5$, and $x_2 = 1.0$, (d) the leading-depression N-wave initial form with $H_1 = 0.006$, $c_1 = 0.4444$, $x_1 = 4.1209$, $H_2 = 0.018$, $c_2 = 4.0$, and $x_2 = 1.6384$.

3.1. *Comparison with Carrier et al.* (*2003*)

Carrier *et al.* (2003) considered four different initial wave profiles using exponential functions, i.e. a Gaussian initial waveform

$$\eta_G(x, 0) = H_1 \exp(-c_1(x - x_1)^2), \tag{3.1}$$

a negative Gaussian initial waveform which can be expressed as $-\eta_G(x, t)$ and two N-wave forms:

$$\eta_N(x, 0) = H_1 \exp(-c_1(x - x_1)^2) - H_2 \exp(-c_2(x - x_2)^2). \tag{3.2}$$

The following initial profiles can be obtained in the transform space after using the linearized form of the transformation for the spatial variable:

$$\eta_G(\sigma, 0) = H_1 \exp\left(-\tfrac{1}{256}c_1(\sigma^2 - \sigma_1^2)^2\right), \tag{3.3}$$

$$\eta_N(\sigma, 0) = H_1 \exp\left(-\tfrac{1}{256}c_1(\sigma^2 - \sigma_1^2)^2\right) - H_2 \exp\left(-\tfrac{1}{256}c_2(\sigma^2 - \sigma_2^2)^2\right), \tag{3.4}$$

which respectively lead to

$$\Phi_G(\sigma) = -\tfrac{1}{16}H_1 c_1(\sigma^2 - \sigma_1^2) \exp\left(-\tfrac{1}{256}c_1(\sigma^2 - \sigma_1^2)^2\right), \tag{3.5}$$

$$\Phi_N(\sigma) = -\tfrac{1}{16}H_1 c_1(\sigma^2 - \sigma_1^2) \exp\left(-\tfrac{1}{256}c_1(\sigma^2 - \sigma_1^2)^2\right)$$
$$+ \tfrac{1}{16}H_2 c_2(\sigma^2 - \sigma_2^2) \exp\left(-\tfrac{1}{256}c_2(\sigma^2 - \sigma_2^2)^2\right). \tag{3.6}$$

Figure 2 compares the initial waveforms defined in the physical space with those resulting from the nonlinear solution. The linearized form of the spatial variable in the definition of the initial waveforms gives a satisfactory comparison. Figure 3 presents the evolution of these initial waveforms. Also, shoreline runup–rundown motions and velocities calculated from (2.7) and (2.9) are compared (figure 4). As hoped, both formulations produce identical results. Equation (2.10) also gives a satisfactory comparison except for case (c) for which $\Phi(0)$ is not small. Table 1 compares flow extrema between the present study and the results of Carrier *et al.* (2003). The numbers are identical.

Carrier *et al.* (2003) observed that the maximum runup height of a positive Gaussian initial waveform is identical to the minimum rundown of a negative Gaussian wave.
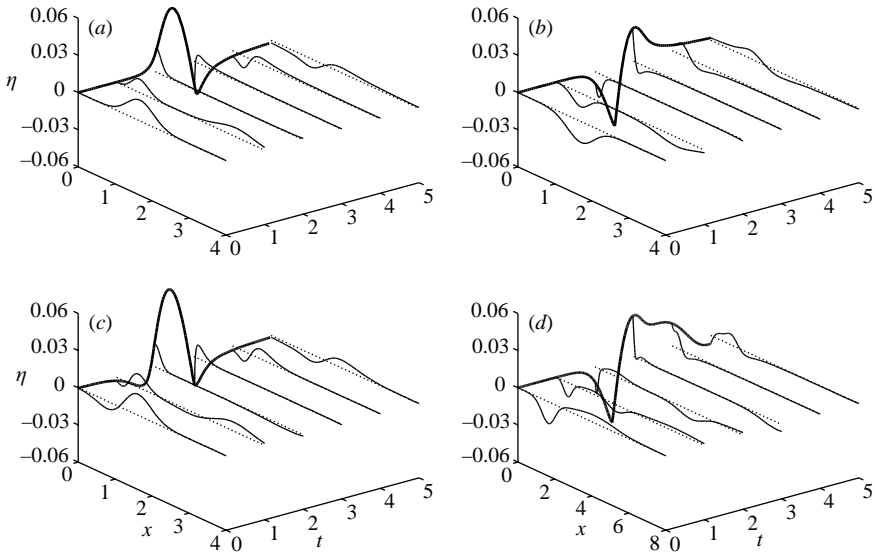
FIGURE 3. Spatial and temporal variations of the water surface elevations including shoreline motions for the four initial waveforms provided by Carrier *et al.* (2003). The nonlinear solution is obtained with the numerical integration of (2.3) using (2.4a–d) and (2.5a). Refer to the caption of the figure 2 for the initial conditions.
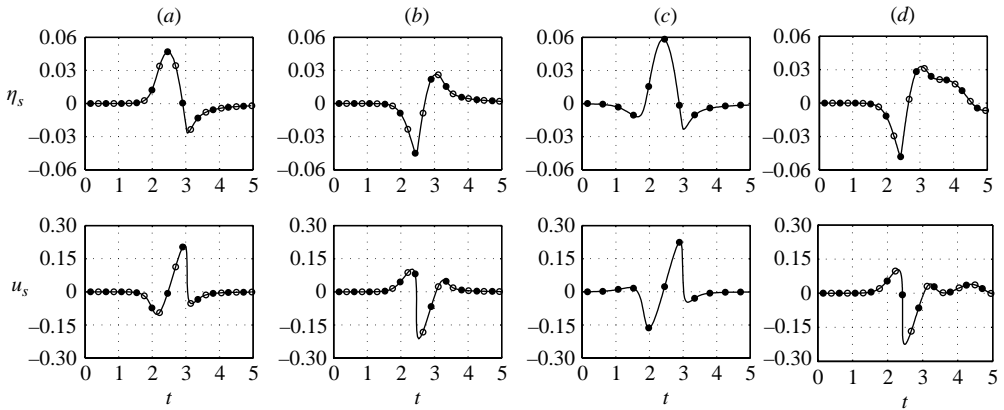

FIGURE 4. Temporal variations of the shoreline runup–rundown motions and velocities. The solid line is based on the numerical integration of (2.7) while the dots and circles represent the result from (2.9) and (2.10) respectively. Refer to the caption of the figure 2 for the initial conditions. The results of (2.10) are not presented for case (c) since it does not provide the good estimate of the quantities presented.

They concluded that "This coincidence may be interpreted as the extreme shoreline location computed by fully nonlinear theory being identical to those predicted by linear theory, whereas the shoreline trajectories and waveforms are different.... Although their [cases (a) and (b)] run-up and run-down processes are different, their extreme values in velocity u and momentum flux f [$= (x + \eta)u^2$ per unit breadth] turn out to be identical.... It is emphasized that the mirror images in the extreme

	Case (*a*)	Case (*b*)	Case (*c*)	Case (*d*)
Initial wave heights	0.0170 (0.0170)	−0.0170 (−0.0170)	0.0172 (0.0173)	−0.0175 (−0.0175)
Maximum runup	0.0470 (−0.0470)	0.0268 (−0.0268)	0.0583 (−0.0583)	0.0328 (−0.0328)
Minimum rundown	−0.0268 (0.0268)	−0.0470 (0.0470)	−0.0235 (0.0235)	−0.0484 (0.0484)
Maximum shoreward velocity	−0.103 at $x=-0.0259$ (−0.103 at $x=-0.0260$)	−0.213 at $x=0.0333$ (−0.213 at $x=0.0333$)	−0.163 at $x=-0.0166$ (−0.1634 at $x=-0.0167$)	−0.225 at $x=0.0351$ (−0.225 at $x=0.0348$)
Maximum seaward velocity	0.213 at $x=0.0121$ (0.213 at $x=0.0122$)	0.103 at $x=0.0364$ (0.103 at $x=0.0365$)	0.226 at $x=0.0060$ (0.226 at $x=0.00666$)	0.104 at $x=0.0371$ (0.104 at $x=0.0370$)

TABLE 1. Comparison of some extreme values with those of Carrier *et al.* (2003) given in parentheses. Refer to the caption of the figure 2 for the cases presented here. Note that there is a sign difference between the maximum runup–minimum rundown values, since Carrier *et al.* (2003) provide penetration distances rather than runup–rundown values.

magnitudes of u, ψ $[= \eta + \frac{1}{2}u^2]$, and f do not relate to the well-known equivalence in the maximum run-up penetration between the linear and nonlinear theories ...." This observation can be explained with the method presented here: Consider initial waveforms for leading-elevation, $\eta_e(x, 0)$ and -depression, $\eta_d(x, 0)$ N-waves. Given $\eta_e(x, 0) = - \eta_d(x, 0)$, then $\Phi_e(\sigma) = - \Phi_d(\sigma)$ implies $\phi_e(\sigma, \lambda) = - \phi_d(\sigma, \lambda)$ from (2.3); $u = \phi_\sigma/\sigma$ will result in the extreme values of u for the leading-elevation and -depression initial waveforms being the inverse of each, i.e. $(u_e)_{\max} = - (u_d)_{\min}$. Since $u = 0$ at the extreme values of η, $\phi_e(\sigma, \lambda) = - \phi_d(\sigma, \lambda)$ will result in $(\eta_e)_{\max} = - (\eta_d)_{\min}$. However, following the transformation to the physical variables through (2.4*c, d*) the spatial and temporal variations of u will be different, as well as for η.

3.2. *Solitary wave initial condition*

A solitary wave which is initially located at $x = x_i$ with the wave amplitude H is given by $\eta(x, 0) = H \operatorname{sech}^2[\gamma_s(x - x_i)]$ where $\gamma_s = \sqrt{\frac{3}{4}H}$. In (σ, λ)-space it takes the form $\eta(\sigma, 0) = H \operatorname{sech}^2[\frac{1}{16}\gamma_s(\sigma^2 - \sigma_i^2)]$. Here $x_i \cong \frac{1}{16}\sigma_i^2$ at $\lambda = t = 0$. The initial condition at $\lambda = 0$ implies that $\Phi(\sigma) = -H\gamma_s \operatorname{sech}^2[\frac{1}{16}\gamma_s(\sigma^2 - \sigma_i^2)] \tanh[\frac{1}{16}\gamma_s(\sigma^2 - \sigma_i^2)]$. This is then used in (2.3) together with (2.4*a–d*) to evaluate the entire flow field in (x, t)-space.

3.3. *N-wave initial conditions*

Tadepalli & Synolakis (1994) used a step-function travelling displacement at the seafloor and studied the canonical problem for N-wave generation, propagation and runup. They conjectured different types of initial N-wave profiles by considering contemporaneous tsunami events such as in Nicaragua 1992 and East Java 1994 which substantiated by anecdotal reports that tsunamis might appear as leading-depression waves. Also, landslide-generated waves over a slope will generate a leading-depression wave propagating shoreward and an offshore-propagating leading-elevation wave (Liu, Lynett & Synolakis 2003). Here two of the definitions of Tadepalli & Synolakis (1994) will be considered.

3.3.1. *Leading-depression isosceles N-wave initial condition*

Tadepalli & Synolakis (1994) considered an N-wave class with leading-depression and -elevation waves of the same height and at a constant separation distance, with initial surface profile

$$\eta(x,0) = \tfrac{3}{2}\sqrt{3}\,H\,\mathrm{sech}^2[\gamma_i(x - x_i)]\tanh[\gamma_i(x - x_i)], \quad \gamma_i = \tfrac{3}{2}\sqrt{\sqrt{\tfrac{3}{4}}H}, \qquad (3.7)$$

where x_i defines the initial location of the wave and H is the initial wave height. In (σ, λ)-space, the leading-depression isosceles N-wave initial profile takes the form

$$\eta(\sigma,0) = \tfrac{3}{2}\sqrt{3}\,H\,\mathrm{sech}^2\left[\tfrac{1}{16}\gamma_i\left(\sigma^2 - \sigma_i^2\right)\right]\tanh\left[\tfrac{1}{16}\gamma_i\left(\sigma^2 - \sigma_i^2\right)\right], \qquad (3.8)$$

where $x_i \cong \tfrac{1}{16}\sigma_i^2$ at $\lambda = t = 0$. Equation (3.8) leads to

$$\Phi(\sigma) = \tfrac{3}{4}\sqrt{3}\,H\gamma_i\left\{2 - \cosh\left[\tfrac{1}{8}\gamma_i\left(\sigma^2 - \sigma_i^2\right)\right]\right\}\mathrm{sech}^4\left[\tfrac{1}{16}\gamma_i\left(\sigma^2 - \sigma_i^2\right)\right]. \qquad (3.9)$$

Once $\Phi(\sigma)$ is known, the entire flow field can be evaluated from equations (2.4*a, b*). Back transformation to the physical space is straightforward using (2.4*c, d*).

3.3.2. *Generalized N-wave initial condition*

Tadepalli & Synolakis (1994) considered another type of N-wave with a leading-depression wave followed by an elevation wave, naming it a generalized N-wave, in the form of

$$\eta(x,0) = \varepsilon H(x - x_2)\mathrm{sech}^2[\gamma_g(x - x_1)], \quad \gamma_g = \sqrt{\tfrac{3}{4}H}, \qquad (3.10)$$

where ε is a scaling parameter. Following the proposed linearization, the initial wave profile is given in the transform space as

$$\eta(\sigma,0) = \tfrac{1}{16}\varepsilon H\left(\sigma^2 - \sigma_2^2\right)\mathrm{sech}^2\left[\tfrac{1}{16}\gamma_g\left(\sigma^2 - \sigma_1^2\right)\right], \qquad (3.11)$$

which leads to the following equation for $\Phi(\sigma)$:

$$\Phi(\sigma) = \tfrac{1}{16}\varepsilon H\left\{8 - \gamma_g(\sigma^2 - \sigma_2^2)\tanh\left[\tfrac{1}{16}\gamma_g\left(\sigma^2 - \sigma_1^2\right)\right]\right\}\mathrm{sech}^2\left[\tfrac{1}{16}\gamma_g\left(\sigma^2 - \sigma_1^2\right)\right]. \quad (3.12)$$

Again, once $\Phi(\sigma)$ is known, the entire flow field can be resolved.

Several cases are considered here and results are presented in figure 5 with examples of solitary, leading-depression N-wave, and leading-elevation N-wave initial forms. Reluctant to draw a conclusion from a few data points and noting that Synolakis (1987) and Tadepalli & Synolakis (1994) solved the canonical problem using the linear shallow-water wave equation with slightly different normalization and introducing the initial waveforms over the constant-depth segment, the following observations are made.

Synolakis (1987) derived an analytical expression for the maximum runup of a solitary wave as $R = 2.831\sqrt{\cot\beta}\,H^{5/4}$. Tadepalli & Synolakis (1994) showed that for a leading-elevation isosceles N-wave $R = 3.86\sqrt{\cot\beta}\,H^{5/4}$ and that for a leading-depression generalized N-wave $R = 2.831\varepsilon\sqrt{\cot\beta}\,H^{5/4}[|x_1 - x_2 - 0.366/\gamma_g| + 0.618/\gamma_g]$. Figure 5(*j*) presents that maximum runup of solitary wave follows $R \sim H^{5/4}$ as analytically derived by Synolakis (1987). Figure 5(*k*) shows that maximum runup of the leading-elevation isosceles N-waves also varies as $H^{5/4}$, as given in Tadepalli & Synolakis (1994), and that maximum runup of the leading-depression isosceles N-waves also varies with $H^{5/4}$. It should also noted here that because of the maximum runup–minimum rundown invariance between the leading-elevation and -depression
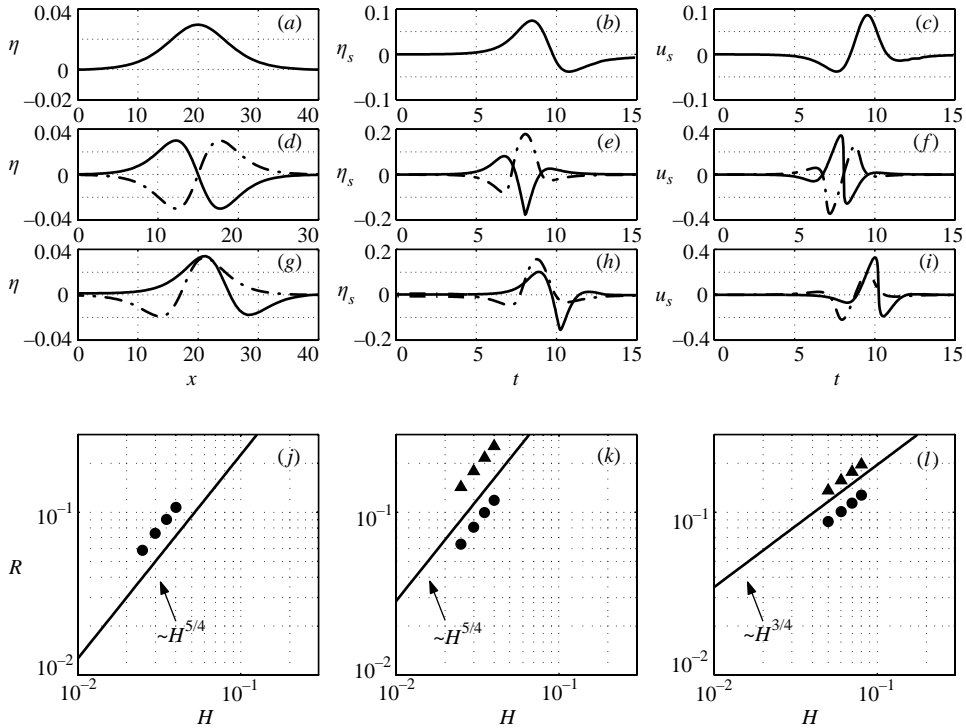
FIGURE 5. The runup–rundown characteristics of (a–c) solitary ($H = 0.03$, $x_i = 20$), (d–f) leading-depression ($H = 0.03$, $x_i = 15$) and -elevation ($\eta_e(x, 0) = -\eta_d(x, 0)$) isosceles N-wave, and (g–i) leading-depression ($H = 0.06$, $\varepsilon = 0.2$, $x_1 = 18$, and $x_2 = 17$) and -elevation ($H = 0.06$, $\varepsilon = 0.2$, $x_1 = 24.20$, and $x_2 = 25.20$) generalized N-wave initial waveforms. The dash-dotted and solid lines represent the quantities for the leading-depression and -elevation initial waveforms, and the triangles and circles represent their maximum runup, respectively. (a, d, g) The initial waveform resulting from nonlinear solution. (b, e, h) Temporal variation of the shoreline motion. (c, f, i) Temporal variation of the shoreline velocity. (j) The maximum runup of the solitary waves with $H = 0.04$, 0.035, 0.03, and 0.025 at $x_i = 20$. (k) The maximum runup of the leading-depression and -elevation isosceles N-waves with $H = 0.04$, 0.035, 0.03, and 0.025 at $x_i = 15$. (l) The maximum runup of the leading-depression generalized N-waves with $H = 0.08$, 0.07, 0.06, and 0.05, $\varepsilon = 0.2$, $x_1 = 18$, and $x_2 = 17$ and the maximum runup of leading-elevation generalized N-waves with $\varepsilon = 0.2$, $x_1 - x_2 = -1$, and $x_1 = 23.24$, 23.66, 24.20, and 24.88 for $H = 0.08$, 0.07, 0.06, and 0.05 respectively. Both initial waveforms have the same maximum amplitude at the same location with these parameters.

wave results, the same scaling is valid for minimum rundown values for both initial waveforms. The runup variation on the leading wave height is approximately $R \sim H^{3/4}$ for the leading-depression generalized N-wave, as in figure 5(l). The approximate absolute upper bound for a leading-depression generalized N-wave presented by Tadepalli & Synolakis (1994) also implies the same variation, since $1/\gamma_g \sim H^{-1/2}$. Moreover, it is observed that maximum runup of the leading-depression isosceles and generalized N-waves is higher than that of leading-elevation N-waves as discussed in Tadepalli & Synolakis (1994) and Carrier *et al.* (2003).

It should be added that the solution presented here cannot be evaluated when the Jacobian of the transformation, $J = x_\sigma \, t_\lambda - x_\lambda \, t_\sigma$, breaks down. Even though the transformation might become singular at certain points, the solution can still be obtained at other points, since local integration can be performed without prior

knowledge of the dependent variables, unlike in numerical methods. This feature is discussed in detail in Synolakis (1987) and Carrier *et al.* (2003).

4. Conclusions

The difficulty with the Carrier–Greenspan transformation, namely deriving an equivalent initial condition over the transform space for a given initial wave profile in the physical space, is resolved. Physically realistic initial waveforms can be represented in the transform space and evolution and the shoreline motion–velocity can be estimated through numerical integration. The proposed analysis appears simpler than in Carrier *et al.* (2003) and produces identical results. Unlike Carrier *et al.* (2003), this analysis does not resort to solving singular elliptic integrals.

Liu, Synolakis & Yeh (1991) wrote "Interestingly, even though many assumptions of the shallow-water wave theory are violated in the surf zone, certain quantitative and qualitative comparisons of its predictions with the experimental or field data often produce good agreement: this is puzzling." Titov & Synolakis (1995) validated this claim through detailed comparisons of numerical solutions of the nonlinear shallow-water wave equations with laboratory data and the boundary value problem solution of the nonlinear shallow-water wave equations of Synolakis (1987). Based on the "quantitative and qualitative" prediction power of the nonlinear shallow-water wave equations, the method outlined here may be useful to assess the impact of long waves generated by seafloor displacements and to validate numerical codes. However, the boundary value problem solution of Synolakis (1987) is more convenient when comparing time series from laboratory data with analytical predictions. Moreover, the present work shows that the initial value problem and boundary value problem predictions converge to the same power law for the variation of the runup on the leading wave height.

REFERENCES

CARRIER, G. F. & GREENSPAN, H. P. 1958 Water waves of finite amplitude on a sloping beach. *J. Fluid Mech.* **4**, 97–109.

CARRIER, G. F., WU, T. T. & YEH, H. 2003 Tsunami runup and drawdown on a plane beach. *J. Fluid Mech.* **475**, 449–461.

GRADSHTEYN, I. S. & RYZHIK, I. M. 1994 *Table of Integrals, Series, and Products*. Academic.

LIU, P. L.-F., SYNOLAKIS, C. E. & YEH, H. H. 1991 The international workshop on long-wave runup. *J. Fluid Mech.* **229**, 675–688.

LIU, P. L.-F., LYNETT, P. & SYNOLAKIS, C. E. 2003 Analytical solutions for forced long waves on a sloping beach. *J. Fluid Mech.* **478**, 101–109.

PELINOVSKY, E. 1995 Nonlinear hyperbolic equations and run-up of huge sea waves. *Applicable Analysis* **57**, 63–84.

SYNOLAKIS, C. E. 1987 Runup of solitary waves. *J. Fluid Mech.* **185**, 523–545.

SYNOLAKIS, C. E., LIU, P. L.-F., YEH, H. & CARRIER, G. F. 1997 Tsunamigenic seafloor deformations. *Science* **278**, 598–600.

TADEPALLI, S. & SYNOLAKIS, C. E. 1994 The run-up of N-waves on sloping beaches. *Proc. R. Soc. Lond.* A **445**, 99–112.

TITOV, V. V. & SYNOLAKIS, C. E. 1995 Modeling of breaking and nonbreaking long-wave evolution and runup using VTCS-2. *J. Waterway, Port, Coastal, Ocean Engng* **121**, 308–316.

TUCK, E. O. & HWANG, L.-S. 1972 Long wave generation on a sloping beach. *J. Fluid Mech.* **51**, 449–461.